



Journal Homepage: -[www.journalijar.com](http://www.journalijar.com)  
**INTERNATIONAL JOURNAL OF  
 ADVANCED RESEARCH (IJAR)**

Article DOI:10.21474/IJAR01/ 9499  
 DOI URL: <http://dx.doi.org/10.21474/IJAR01/9499>



### RESEARCH ARTICLE

## TRIORGANOTIN PHOSPHONATES POLYMERIC CHAINS– SYNTHESIS, INFRARED, MÖSSBAUER AND SINGLE CRYSTAL CHARACTERIZATION: THE FIRST ORGANOTIN(IV) PH<sub>2</sub> BRIDGED

Mouhamadou Birame Diop<sup>1</sup>, Mouhamadou Sembene Boye<sup>1,2</sup>, Aminata Diassé-Sarr<sup>1</sup>, Libasse Diop<sup>1</sup>, Philippe Guionneau<sup>3</sup> and Thierry Maris<sup>4</sup>.

1. Laboratoire de Chimie Minérale et Analytique (LA.CHI.MI.A.), Département de Chimie, Faculté des Sciences et Techniques, Université Cheikh Anta Diop, Dakar, Sénégal.
2. Département de Physique-Chimie, Faculté des Sciences et Technologies de l'Éducation et de la Formation (FASTEF), Université Cheikh Anta Diop, Dakar, Sénégal.
3. Institut de Chimie de la Matière Condensée de Bordeaux, CNRS-Université de Bordeaux, 87 Avenue du Docteur A. Schweitzer 33608 Pessac, France.
4. Département de Chimie, Université de Montréal, 2900 Boulevard Édouard-Montpetit, Montréal, Québec, Canada, H3C 3J7.

#### Manuscript Info

##### Manuscript History

Received: 06 June 2019  
 Final Accepted: 08 July 2019  
 Published: August 2019

##### Key words:-

triorganotin(IV); phosphonate; PH<sub>2</sub>  
 bridge; infrared; Mössbauer; X-ray  
 crystallography.

#### Abstract

Two triorganotin(IV) phosphonate compounds were isolated and structurally investigated by infrared and Mössbauer spectroscopies and X-ray crystallography. The reaction of trimethyltin(IV) chloride (SnMe<sub>3</sub>Cl) and hexamethylene tetraammonium hydrogen methylphosphonate [CH<sub>3</sub>PO<sub>3</sub>H][N<sub>4</sub>(CH<sub>2</sub>)<sub>6</sub>H] led to the formation of [C<sub>10</sub>H<sub>34</sub>O<sub>4</sub>P<sub>2</sub>Sn<sub>3</sub>] (**1**) which crystallizes in the Monoclinic space group *Pn* with *Z* = 2, *a* = 8.4955 (2) Å, *b* = 11.318 (3) Å, *c* = 11.902 (2) Å, β = 90.9340 (10)° and *V* = 1144.2 (4) Å<sup>3</sup>. An uncommon decomposition of methylphosphonate occurred during the reaction process giving rise to the formation of dimers of [SnMe<sub>3</sub>PH<sub>2</sub>SnMe<sub>3</sub>]<sup>+</sup>. The structure of **1** consists of an anionic chain of [CH<sub>3</sub>PO<sub>3</sub>(SnMe<sub>3</sub>PH<sub>2</sub>SnMe<sub>3</sub>)]<sup>-</sup> linked to [SnMe<sub>3</sub>(H<sub>2</sub>O)]<sup>+</sup> moieties through Sn—O bonds involving the remaining oxygen atoms of the methylphosphonates. In the chain, each SnMe<sub>3</sub> residue is coordinated by one methylphosphonate and one phosphor atom, in a *trans*-trigonal bipyramidal PSnC<sub>3</sub>O geometry. The environment at tin atoms in both SnMe<sub>3</sub> moieties is an octahedron. The methylphosphonate anion is otherwise in a general position and behaves as a tri-coordinating ligand. The reaction of triphenyltin(IV) hydroxide (SnPh<sub>3</sub>OH) and phosphorous acid (HPO(OH)<sub>2</sub>) led to the formation of [C<sub>36</sub>H<sub>31</sub>O<sub>3</sub>PSn<sub>2</sub>] (**2**) which crystallizes in the Monoclinic space group *P2/n* with *Z* = 4, *a* = 11.7966 (4) Å, *b* = 10.1953 (4) Å, *c* = 27.6715 (10) Å, β = 94.600 (2)° and *V* = 3317.3 (2) Å<sup>3</sup>. The structure of **2** is comprised of an anionic chain of [HPO<sub>3</sub>(SnPh<sub>3</sub>)]<sup>-</sup> linked to SnPh<sub>3</sub> moieties through Sn—O bonds involving the remaining oxygen atoms of the hydrogenphosphonates. In the chain the SnPh<sub>3</sub> residues are each one coordinated by two hydrogenphosphonates in a *trans*-trigonal bipyramidal OSnC<sub>3</sub>O arrangement. The geometry at tin atoms within the monocoordinated SnPh<sub>3</sub> moieties connected to the chain is a

**Corresponding Author:-Mouhamadou Birame Diop.**

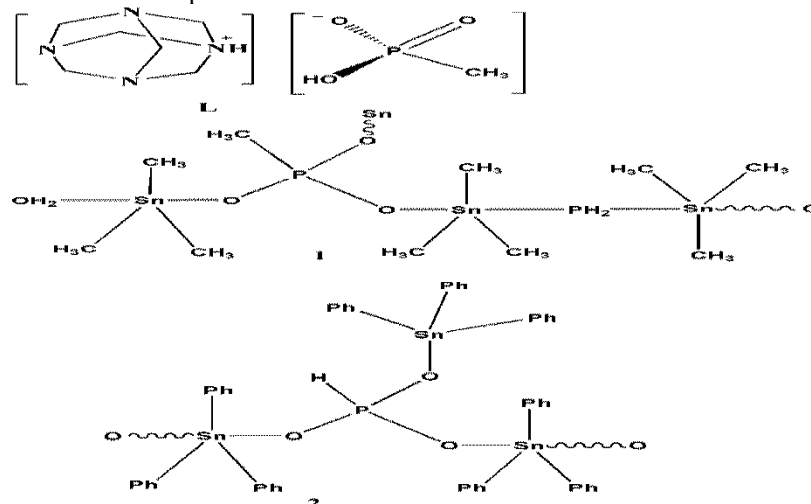
Address:-Laboratoire de Chimie Minérale et Analytique (LA.CHI.MI.A.), Département de Chimie, Faculté des Sciences et Techniques, Université Cheikh Anta Diop, Dakar, Sénégal.

distorted tetrahedron. The hydrogenphosphonate anion is in a general arrangement and behaves as a tri-O-coordinating ligand.

Copy Right, IJAR, 2019.. All rights reserved.

### Introduction:-

Metal phosphonate and organotin(IV) classes of compounds aroused and still arouse a great interest because of the wide properties and applications they display in various fields (Bao and Zheng, 2016; Hamchaoui *et al.*, 2013a; Clearfield and Demadis, 2012; Mao, 2007; Fernandez-Armas *et al.*, 2004a, Mallouk *et al.*, 1996; Cao *et al.*, 1992; Etaiwet *et al.* 2019; Mao *et al.*, 2015; Devendra *et al.*, 2015; Carraher *et al.*, 2019, 2018; Roner *et al.*, 2014). Numerous organic phosphonate compounds were isolated and widely used as anti-HIV, antiviral in AIDS treatment (Troev, 2006). Few organic salt structures involving methylphosphonate anion were reported in the past three decades (Mahmoudkhani and Langer, 2002; Fleck *et al.*, 2000; Paixao *et al.*, 2000; Honle *et al.*, 1990). To date, several hydrogenphosphonate compounds with different metals such as Mn, Co, Ga, Cr, V, Fe, Cd, In and U have earlier been reported in the literature (Ouarsal *et al.*, 2016; Larrea *et al.* 2016; Berrocal *et al.*, 2014; Oh and Burns, 2014; Hamchaoui *et al.*, 2013a, 2013b; Li *et al.*, 2009; Fernandez-Armas *et al.*, 2004a, 2004b). In some of these structures, the hydrogenphosphonate anion behaves as multidirectional synthons. Contributing to widen phosphonate family compounds, the Dakar group has already reported the spectroscopic (Infrared, Mössbauer and NMR) studies of some  $RPO_3(SnPh_3)_2$  ( $R = H$  or  $CH_3$ ) (Diop *et al.*, 1999), the crystal characterization of dibutylammonium bis(hydrogen methylphosphonato- $\kappa$ O)triphenylstannate(IV) (Diop *et al.*, 2012a) as well as numerous phenylphosphonato triphenyltin(IV) crystalline structures which, through hydrogen bonding interactions, exhibit various structures that give rise to supramolecular diverse topologies (Diop *et al.*, 2013a, 2012b, 2011a, 2011b). To the best of our knowledge (CSD version 5.40), very few, only three tin(IV) methylphosphonate and five tin(IV) hydrogenphosphonate containing crystalline compounds are known (Diop *et al.*, 2012a; Ribot *et al.*, 2001; Adair *et al.*, 1998; Chandrasekharet *et al.*, 2003, 2005; Mairychova *et al.*, 2014). The organotin(IV) methylphosphonate cores have discrete structures, monomeric (Diop *et al.*, 2012a) or dimeric (Ribot *et al.*, 2001) with monodentate and bidentate and monodentate anions, respectively. Though, the inorganic tin(IV) methylphosphonate complex is polymeric with tri-O-coordinating ligands. Contrary to the firsts, the organotin(IV) hydrogenphosphonate compounds have a dimeric structure with bidentate ligands (Mairychova *et al.*, 2014) or an hexameric cage structure in a double O-capped cluster with tri-O-coordinating ligands (Chandrasekharet *et al.*, 2003, 2005). Thus, continuing to focus in phosphonate organotin(IV) family compounds, we investigated in this work, in organic solvents, the interactions between a salt of methylphosphonic acid,  $CH_3PO(OH)_2$  and hexamethylene tetraamine (L) and, trimethyltin(IV) chloride in one hand and, phosphorous acid,  $HPO(OH)_2$  and triphenyltin(IV) hydroxide in another hand. These interactions yielded single crystals of compounds 1,  $[SnMe_3(PH_2)SnMe_3][CH_3PO_3][SnMe_3(H_2O)]$  and 2,  $HPO_3(SnPh_3)_2$  (Scheme 1) whose X-ray and spectroscopic characterization are carried out and reported herein.



**Scheme 1:-**Molecular representations of hexamethylene tetraammonium hydrogen methylphosphonate reagent and compounds related to this study.

**Experimental section:-**

Triphenyltin hydroxide,  $\text{SnPh}_3\text{OH}$  (99 % purity) and trimethyltin chloride,  $\text{SnMe}_3\text{Cl}$  (99 % purity), phosphorous acid,  $\text{HPO}(\text{OH})_2$  (99 % purity),  $\text{N}_4(\text{CH}_2)_6$  (99 % purity) and  $\text{CH}_3\text{PO}(\text{OH})_2$  (99 % purity) were purchased from Sigma-Aldrich, Steinheim am Albuch, Germany and were used without any further purification.

Infrared spectra were recorded on a Bruker Vector 22 spectrometer equipped with a Specac Golden Gate<sup>TM</sup> ATR device. [IR abbreviations: (vs) very strong, (s) strong, (m) medium, (br) broad, (sh) shoulder].

Elemental analyses were performed at the Institut de Chimie de la Matière Condensée, Université de Bordeaux, France and at the Institut de Chimie Moléculaire, Université de Bourgogne Franche-Comté, Dijon, France.

<sup>119</sup>Sn Mössbauer data were collected as reported in (Bouâlamet *et al.*, 1991) and in (Diop *et al.*, 2013b), respectively. Mössbauer parameters are given in  $\text{mm}\cdot\text{s}^{-1}$  [Mössbauer abbreviations: Q.S = quadrupole splitting, I.S = isomer shift,  $\Gamma$  = full width at half-height].

**Synthesis and isolation of  $[\text{SnMe}_3(\text{PH}_2)\text{SnMe}_3][\text{CH}_3\text{PO}_3][\text{SnMe}_3(\text{H}_2\text{O})](1)$ :-**

The isolation of **1** follows a two steps procedure. The salt hexamethylene tetraammonium hydrogen methylphosphonate,  $[\text{CH}_3\text{PO}_3\text{H}][\text{N}_4(\text{CH}_2)_6\text{H}](\text{L})$  was first collected as a white powder from reaction between equimolar aqueous solutions of methylphosphonic acid,  $\text{CH}_3\text{PO}(\text{OH})_2$  (600mg, 6.25mmol) and hexamethylene tetraamine,  $\text{N}_4(\text{CH}_2)_6$  (876mg, 6.25mmol). To 15 mL methanol solution of **L** (469mg, 1.98mmol) was added 10 mL dichloromethane solution of  $\text{SnMe}_3\text{Cl}$  (395mg, 1.98mmol). The clear obtained mixture was stirred 2h at room temperature (303K) then submitted to a slow solvent evaporation. After four days of a slow evaporation at room temperature (303K), in a not-controlled atmosphere, colourless crystals (melting point = 386K) suitable for an X-ray analysis were picked up from the solution and were finally characterized as **1**.

**Spectroscopic data:-**

1. IR data ( $\text{cm}^{-1}$ ):  $\nu\text{OH}$  3389(br), 3192(sh),  $\nu\text{PO}_3^{2-}$  1112(s), 1060(s), 995(s),  $\nu\text{PC}$  850(m),  $\nu\text{asSnC}_3$  545(s)
2. Mössbauer parameters ( $\text{mm}\cdot\text{s}^{-1}$ ): IS = 1.47, QS = 3.60,  $\Gamma$  = 0.96

**Elemental Analysis:-**

$[\text{SnMe}_3(\text{PH}_2)\text{SnMe}_3][\text{CH}_3\text{PO}_3][\text{SnMe}_3(\text{H}_2\text{O})]$  (**1**),  $\text{C}_{10}\text{H}_{34}\text{O}_4\text{P}_2\text{Sn}_3$ , [%calculated (%found)]:- C = 18.87 (18.63), H = 5.38 (5.19); yield: 55%

$[\text{CH}_3\text{PO}_3\text{H}][\text{N}_4(\text{CH}_2)_6\text{H}](\text{L})$ , [%calculated (%found)]:- C = 35.60 (35.22), H = 7.25 (7.39), N = 23.72 (23.75); yield: 85%

**Synthesis and isolation of  $[\text{HPO}_3(\text{SnPh}_3)_2]$  (**2**):-**

To 15mL methanol solution of triphenyltin hydroxide,  $\text{SnPh}_3\text{OH}$  (551mg, 1.50mmol) was added an equimolar solution of phosphorous acid,  $\text{HPO}(\text{OH})_2$  (123mg, 1.50mmol) preliminary dissolved in 15mL of methanol, giving rise to a clear solution. The resulting mixture was stirred 2h at room temperature (303K) before being submitted to evaporation. After five days of slow solvent evaporation at room temperature (303K), in a not-controlled atmosphere, colourless crystals, suitable for an X-ray crystallographic analysis grew from the solution and were finally characterized as **2**.

**Spectroscopic data:-**

1. IR data ( $\text{cm}^{-1}$ ):  $\nu\text{PH}$  2495 (s),  $\nu\text{PO}_3^{2-}$  1132(vs), 1109(vs),  $\delta\text{PH}$  1075(vs),  $\nu\text{CC}$  and  $\nu\text{CH}$  (phenyl groups) 735(vs), 697(s)
2. Mössbauer parameters ( $\text{mm}\cdot\text{s}^{-1}$ ): IS<sub>1</sub> = 1.26, QS<sub>1</sub> = 2.84,  $\Gamma_1$  = 0.89; IS<sub>2</sub> = 1.34, QS<sub>2</sub> = 2.51,  $\Gamma_2$  = 0.92

**Elemental Analysis:-**

$[\text{HPO}_3(\text{SnPh}_3)_2]$  (**2**),  $\text{C}_{36}\text{H}_{31}\text{O}_3\text{PSn}_2$ , [%calculated (%found)]:- C = 55.43 (55.77), H = 4.01 (3.98); yield: 75%.

**X-ray crystallography of  $[\text{SnMe}_3(\text{PH}_2)\text{SnMe}_3][\text{CH}_3\text{PO}_3][\text{SnMe}_3(\text{H}_2\text{O})](1)$ :-**

A crystal of approximate dimensions 0.25×0.12×0.12 mm was used for data collection. The X-ray crystallographic data were collected using a Nonius KappaCCD diffractometer at  $T = 150$  (2) K. Data were measured using  $\varphi$  and  $\omega$  scans using  $\text{MoK}\alpha$  radiation ( $\lambda = 0.71073 \text{ \AA}$ ) using a collection strategy to obtain a hemisphere of unique data determined by COLLECT (Nonius, 2003). Cell parameters were determined and refined using the

SCALEPACK (Otwinowski and Minor, 1997). Data were corrected for absorption by the empirical absorption correction using DENZO (Otwinowski and Minor, 1997). The structure was solved using SHELXS (Sheldrick, 2008) and the structure refined using least-squares minimization SHELXL (Sheldrick, 2008).

Programs used for the representation of the molecular and crystal structures: Olex2 (Dolomanov *et al.*, 2009) and Mercury (Macrae *et al.*, 2008). The Crystallographic data and experimental details for structural analyses are summarized in Table 1. Selected bond lengths and angles are listed in Tables 2 and 3, respectively.

CCDC 805143 (1) contains the supplementary crystallographic data for this paper. These data can be obtained free of charge from the Cambridge Crystallographic Data Centre via [www.ccdc.cam.ac.uk/data\\_request/cif](http://www.ccdc.cam.ac.uk/data_request/cif), or by emailing [data\\_request@ccdc.cam.ac.uk](mailto:data_request@ccdc.cam.ac.uk), or by contacting The Cambridge Crystallographic Data Centre, 12 Union Road, Cambridge CB2 1EZ, UK; fax: +44(0)1223-336033.

#### X-ray crystallography of [HPO<sub>3</sub>(SnPh<sub>3</sub>)<sub>2</sub>] (2):-

A crystal of approximate dimensions 0.32×0.23×0.12 mm was used for data collection. The X-ray crystallographic data were collected using a Bruker Venture Metaljet diffractometer, at  $T = 100$  K. Data were measured using  $\varphi$  and  $\omega$  scans using GaK $\alpha$  radiation ( $\lambda = 1.34139$  Å) using a collection strategy to obtain a hemisphere of unique data determined by Apex2 (Bruker AXS Inc., Madison, WI 53719-1173., 2013). Cell parameters were determined and refined using the SAINT program (SAINT (2013) V8.35A). Data were corrected for absorption by multi-scan absorption correction using SADABS2014/5 (Krause *et al.*, 2015). The structure was solved using Olex2 (Dolomanov *et al.*, 2009) and the structure refined using least-squares minimization SHELXL (Sheldrick, 2008).

Programs used for the representation of the molecular and crystal structures: Olex2 (Dolomanov *et al.*, 2009) and Mercury (Macrae *et al.*, 2008). The Crystallographic data and experimental details for structural analyses are summarized in Table 1. Selected bond lengths and angles are listed in Tables 2 and 3, respectively.

CCDC 1917005 (2) contains the supplementary crystallographic data for this paper. These data can be obtained free of charge from the Cambridge Crystallographic Data Centre via [www.ccdc.cam.ac.uk/data\\_request/cif](http://www.ccdc.cam.ac.uk/data_request/cif), or by emailing [data\\_request@ccdc.cam.ac.uk](mailto:data_request@ccdc.cam.ac.uk), or by contacting The Cambridge Crystallographic Data Centre, 12 Union Road, Cambridge CB2 1EZ, UK; fax: +44(0)1223-336033.

**Table 1:**-Crystal data and structure refinement for compounds (1) and (2)

Parameters	Compound	
	(1)	(2)
Empirical formula	C <sub>10</sub> H <sub>34</sub> O <sub>4</sub> P <sub>2</sub> Sn <sub>3</sub>	C <sub>36</sub> H <sub>31</sub> O <sub>3</sub> PSn <sub>2</sub>
Formula weight	636.38	779.96
Temperature	150 (2) K	100 K
Wavelength	0.71073 Å	1.34139 Å
Crystal system	Monoclinic	Monoclinic
Space group	<i>Pn</i>	<i>P2/n</i>
Unit cell dimensions	a = 8.4955 (2) Å $\alpha = 90^\circ$ b = 11.318 (3) Å $\beta = 90.934(1)^\circ$ c = 11.902 (2) Å $\gamma = 90^\circ$	a = 11.7966 (4) Å $\alpha = 90^\circ$ b = 10.1953 (4) Å $\beta = 94.600 (2)^\circ$ c = 27.6715 (10) Å $\gamma = 90^\circ$
Volume	1144.2 (4) Å <sup>3</sup>	3317.3(2) Å <sup>3</sup>
Z	2	4
Calculated density	1.847 g cm <sup>-3</sup>	1.562 g cm <sup>-3</sup>
Absorption coefficient	3.394 mm <sup>-1</sup>	8.628 mm <sup>-1</sup>
F(000)	612	1544
Crystal size	0.25 × 0.12 × 0.12 mm <sup>3</sup>	0.32 × 0.23 × 0.12 mm <sup>3</sup>
Theta range for data collection	2.48–34.96°	3.271–60.733°
Limiting indices	-13 ≤ <i>h</i> ≤ 13, -18 ≤ <i>k</i> ≤ 18, -19 ≤ <i>l</i> ≤ 19	-14 ≤ <i>h</i> ≤ 15, -13 ≤ <i>k</i> ≤ 13, -35 ≤ <i>l</i> ≤ 31
Reflections collected/unique	16601/9234	45257/7609
R <sub>int</sub>	0.0215	0.0537

Absorption correction	Empirical	Multi-scan
Max. and min. transmission	0.6862 and 0.4841	0.3107 and 0.0900
Refinement method	Full-matrix least-squares on $F^2$	Full-matrix least-squares on $F^2$
Data/restraints/parameters	9234/2/182	7609/0/385
Goodness-of-fit on $F^2$	1.034	1.043
Final R indices ( $I > 2\sigma(I)$ )	$R_1 = 0.0229$ , $wR_2 = 0.0539$	$R_1 = 0.1014$ , $wR_2 = 0.0356$
R indices (all data)	$R_1 = 0.0259$ , $wR_2 = 0.0524$	$R_1 = 0.1007$ , $wR_2 = 0.0363$
Largest diff. peak and hole	0.891 and $-0.445 \text{ e } \text{\AA}^{-3}$	1.835 and $-0.804 \text{ e } \text{\AA}^{-3}$

$w = 1/[s^2(F_o^2) + (0.0257P)^2 + 0.0154P]$  for **1** and  $w = 1/[s^2(F_o^2) + (0.0571P)^2 + 6.2522P]$  for **2**, where  $P = (F_o^2 + 2F_c^2)/3$ .

**Table 2:-** Selected bond lengths(Å) for **1** and **2**

(1)		(2)	
Atom—Atom	Bond length	Atom—Atom	Bond length
Sn2—C4	2.122 (3)	Sn1—O2 <sup>i</sup>	2.196 (2)
Sn2—C2	2.123 (3)	Sn1—O2	2.196 (2)
Sn2—C3	2.125 (3)	Sn1—C1	2.146 (5)
Sn2—O3	2.1621 (19)	Sn1—C5 <sup>i</sup>	2.134 (3)
Sn2—P2	2.8407 (7)	Sn1—C5	2.134 (3)
Sn1—C6	2.124 (3)	Sn2—O3 <sup>ii</sup>	2.242 (2)
Sn1—C5	2.127 (3)	Sn2—O3	2.242 (2)
Sn1—C7	2.129 (3)	Sn2—C11	2.126 (5)
Sn1—O1	2.1313 (19)	Sn2—C15 <sup>ii</sup>	2.128 (3)
Sn1—O4	2.416 (2)	Sn2—C15	2.128 (3)
Sn3—C10	2.119 (3)	Sn3—O1	2.001 (2)
Sn3—C8	2.124 (3)	Sn3—C21	2.114 (3)
Sn3—C9	2.128 (3)	Sn3—C27	2.120 (3)
Sn3—O2 <sup>i</sup>	2.140 (2)	Sn3—C33	2.121 (3)
Sn3—P2	2.8190 (10)	P1—H1	1.42 (4)
P1—O1	1.512 (2)	P1—O1	1.553 (2)
P1—O2	1.519 (2)	P1—O2	1.502 (2)
P1—O3	1.538 (2)	P1—O3	1.510 (2)
P1—C1	1.786 (3)		
O2—Sn3 <sup>ii</sup>	2.140 (2)		

**Table 3:-** Selected angles(°) for **1** and **2**

(1)		(2)	
Atom-atom-atom	Angle value	Atom-atom-atom	Angle value
C4—Sn2—C2	122.58 (13)	O2 <sup>i</sup> —Sn1—O2	177.03 (12)
C4—Sn2—C3	117.54 (15)	C1—Sn1—O2 <sup>i</sup>	91.48 (6)
C2—Sn2—C3	118.05 (13)	C1—Sn1—O2	91.48 (6)
C4—Sn2—O3	94.18 (10)	C5—Sn1—O2	85.89 (10)
C2—Sn2—O3	96.54 (10)	C5 <sup>i</sup> —Sn1—O2	92.61 (10)
C3—Sn2—O3	92.68 (10)	C5—Sn1—O2 <sup>i</sup>	92.61 (10)
C4—Sn2—P2	85.82 (9)	C5 <sup>i</sup> —Sn1—O2 <sup>i</sup>	85.89 (10)
C2—Sn2—P2	86.18 (8)	C5—Sn1—C1	120.39 (8)
C3—Sn2—P2	84.45 (9)	C5 <sup>i</sup> —Sn1—C1	120.39 (9)
O3—Sn2—P2	176.74 (5)	C5 <sup>i</sup> —Sn1—C5	119.22 (17)
C6—Sn1—C5	118.83 (14)	O3 <sup>ii</sup> —Sn2—O3	178.22 (13)
C6—Sn1—C7	119.86 (14)	C11—Sn2—O3 <sup>ii</sup>	90.89 (6)
C5—Sn1—C7	119.90 (15)	C11—Sn2—O3	90.89 (6)
C6—Sn1—O1	96.92 (11)	C11—Sn2—C15 <sup>ii</sup>	120.12 (9)
C5—Sn1—O1	93.34 (11)	C11—Sn2—C15	120.12 (9)
C7—Sn1—O1	91.63 (11)	C15 <sup>ii</sup> —Sn2—O3 <sup>ii</sup>	91.42 (10)

C6—Sn1—O4	85.33 (11)	C15 <sup>ii</sup> —Sn2—O3	87.69 (10)
C5—Sn1—O4	86.63 (10)	C15—Sn2—O3 <sup>ii</sup>	87.69 (10)
C7—Sn1—O4	86.17 (11)	C15—Sn2—O3	91.42 (11)
O1—Sn1—O4	177.44 (10)	C15 <sup>ii</sup> —Sn2—C15	119.76 (18)
C10—Sn3—C8	120.71 (17)	O1—Sn3—C21	110.27 (11)
C10—Sn3—C9	120.70 (17)	O1—Sn3—C27	99.28 (11)
C8—Sn3—C9	117.31 (16)	O1—Sn3—C33	105.40 (12)
C10—Sn3—O2 <sup>i</sup>	91.46 (11)	C21—Sn3—C27	110.70 (13)
C8—Sn3—O2 <sup>i</sup>	94.99 (10)	C21—Sn3—C33	113.76 (13)
C9—Sn3—O2 <sup>i</sup>	94.92 (10)	C27—Sn3—C33	116.18 (12)
C10—Sn3—P2	85.40 (10)		
C8—Sn3—P2	87.46 (9)		
C9—Sn3—P2	85.86 (9)		
O2 <sup>i</sup> —Sn3—P2	176.71 (5)		

Symmetry codes: for **1**: (i)  $x+1/2, -y, z-1/2$ ; (ii)  $x-1/2, -y, z+1/2$ , for **2**: (i)  $-x+1/2, y, -z+3/2$ ; (ii)  $-x+3/2, y, -z+3/2$

### Results and discussion:-

The infrared spectrum of **1** exhibits a broad band at  $3389\text{ cm}^{-1}$  with a shoulder at  $3192\text{ cm}^{-1}$  assigned to  $\nu\text{OH}$  vibrations involving the water molecule (Nakamoto, 1997). Vibration bands located at  $1112, 1060$  and  $995\text{ cm}^{-1}$  correspond to  $\nu\text{PO}_3^{2-}$  vibrations while that at  $850\text{ cm}^{-1}$  is attributed to the  $\nu\text{PC}$  corroborating presence of the methylphosphonate anion. It is noteworthy to outline absence of a band about  $515\text{--}520\text{ cm}^{-1}$  that may be attributed to  $\nu\text{SnC}_3$  vibration, and presence of a band at  $545\text{ cm}^{-1}$  that is assigned to  $\nu\text{asSnC}_3$  vibrations, indicating a planar  $\text{SnC}_3$  group (Nakamoto, 1997). Tetrahedral tin(IV) centre has a quadrupole splitting about  $2.89\text{ mm.s}^{-1}$  (Bancroft and Platt, 1972; Parish, 1984). Thus, the quadrupole splitting value higher than  $2.89\text{ mm.s}^{-1}$ , is in accordance with coordination at tin atom. The value of  $3.60\text{ mm.s}^{-1}$  is in the range of pentacoordinated tin centres (Bancroft and Platt, 1972; Parish, 1984) in a trigonal bipyramidal arrangement.

The complex **1** which crystallizes in the monoclinic  $Pn$  space group as colourless prism-like crystal, results from a decomposition (cleavage and formation of new bonds) process over the hydrogen methylphosphonate anion of Lused as starting material, when the reaction is carried out in a 3:2 methanol/dichloromethane mixture and in a non-controlled atmosphere. In the past, the in-situ formation of hydrogenphosphonate,  $\text{HPO}_3^{2-}$  from a P—O bond cleavage decomposition has been evidenced (Chandrasekhar *et al.*, 2003). In this compound, the formation of the  $[\text{PH}_2]^-$  is owed to a decomposition, P—O and P—C bonds cleavage. A molecular view of the asymmetric unit is depicted in Fig. 1. Present in **1** is the  $[\text{PH}_2]^-$  bridging anion connecting two  $\text{SnMe}_3$  moieties.

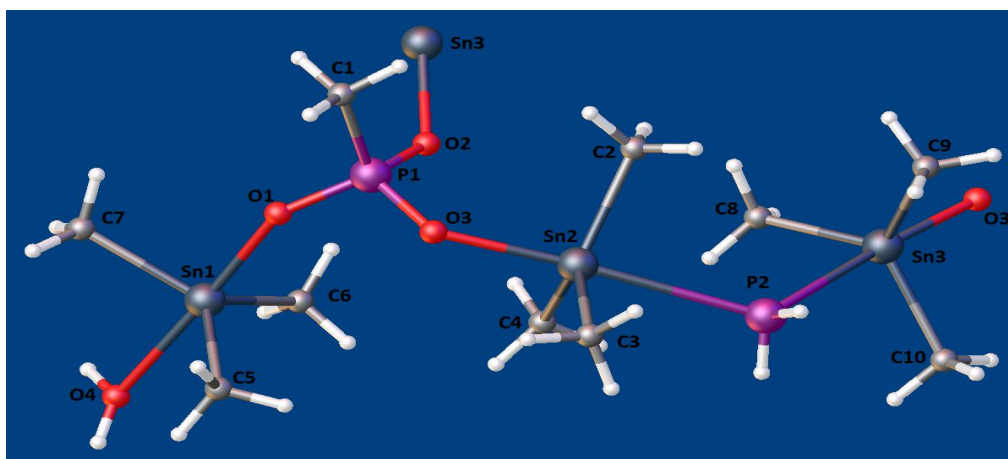


**Fig 1:-** Molecular structure of  $[\text{SnMe}_3(\text{PH}_2)\text{SnMe}_3][\text{CH}_3\text{PO}_3][\text{SnMe}_3(\text{H}_2\text{O})]$  (**1**) showing 50% probability ellipsoids and the crystallographic numbering scheme.

Within the structure of **1** is described an infinite ionic chain of  $[\text{CH}_3\text{PO}_3(\text{SnMe}_3\text{PH}_2\text{SnMe}_3)]^-$  with methylphosphonate anion bridges. To this chain are then linked aquatrimethyltin(IV),  $[\text{SnMe}_3\text{H}_2\text{O}]^+$  cations via the

third remaining phosphonate oxygen atoms through Sn—O bonds (Figs. 2 and 3). The methylphosphonate dianion behaves as a tri O-coordinating ligand. The SnMe<sub>3</sub> residues are *trans*-coordinated, the environment around the tin(IV) atom being trigonal bipyramidal (tbp). Thus, in the *trans*-coordinated SnMe<sub>3</sub> moiety the methyl groups occupy the equatorial positions and the apical positions are occupied by a phosphor atom from the [PH<sub>2</sub>]<sup>-</sup> bridge and an oxygen atom from a methylphosphonate anion for Sn2 and Sn3 while for Sn1 the apical positions are occupied by two oxygen atoms; one from the methylphosphonate and another from the water molecule of crystallization which complete the tbp coordination sphere at tin atom. The sum of the angles at tin centres equal to 358.59°, 358.17° and 358.72° indicate almost planar SnC<sub>3</sub> groups; tin atoms are slightly out the C<sub>3</sub> planes.

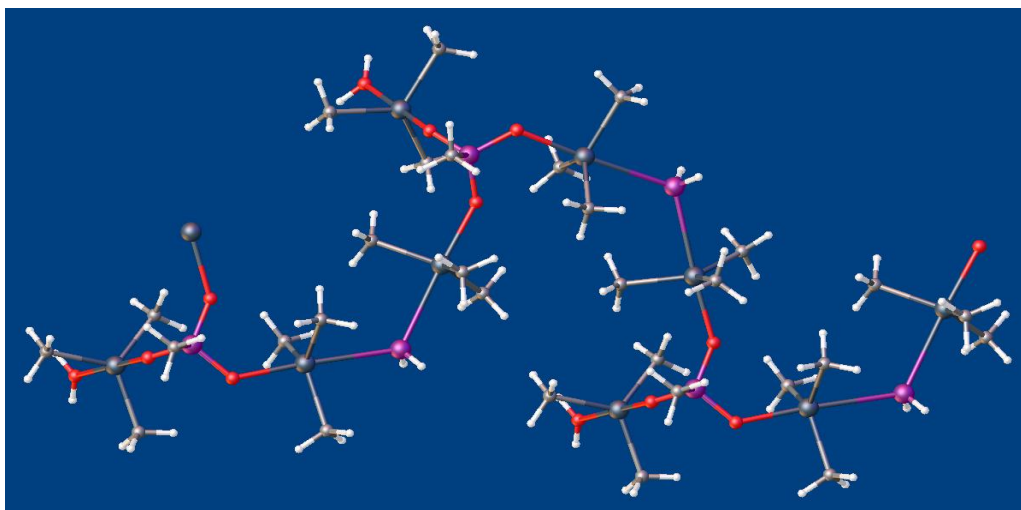


**Fig 2:**-Molecular structure of **1** showing the infinite ionic chain and [SnMe<sub>3</sub>(H<sub>2</sub>O)]<sup>+</sup> cations set on. Ellipsoids are drawn at 50% probability.

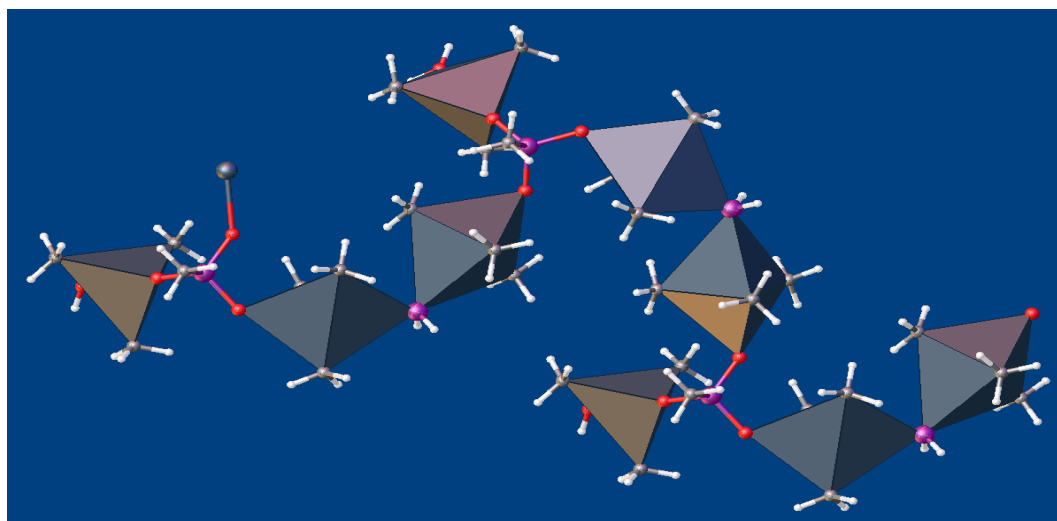


**Fig 3:**-Molecular structure of **1** showing the trigonal bipyramidal polyhedron at tin atoms. Ellipsoids are drawn at 50% probability.

The Sn—C distances are in the range of those found in tbp SnMe<sub>3</sub> moieties (Diop *et al.*, 2013a, 2012b, 2011a). The Sn1—O4 bond of 2.416 (2) Å is longer, weaker than the Sn1—O1 one of 2.1313 (19) Å: these values are in a typical range of Sn—O phosphonate (Diop *et al.*, 2013a, 2012a, 2012b) and Sn—O water (Diop *et al.*, 2015), respectively. Meanwhile the Sn—P bond lengths of 2.8407 (7) and 2.8190 (10) Å are in the range of that previously reported for related PR<sub>2</sub> bridging organotin(IV) compounds (Mertens *et al.*, 1995), they are above those found in organotin(IV) PH bridged and PH<sub>2</sub> terminally bonded (Driess *et al.*, 1995; Hanssgen *et al.*, 1990). The O—Sn—O angle [O1—Sn1—O4 177.44 (10)°] as well as O—Sn—P angles [O3—Sn2—P2 176.74 (5)° and O2<sup>i</sup>—Sn3—P2 176.71 (5)°]

reveal a slight deviation from linearity. The P—O bond distances [from 1.512 (2) to 1.538 (2) Å] and P—C [1.786 (3) Å] are in the range of those found in the literature (Hamchaoui *et al.*, 2013a, 2013b; Diop *et al.*, 2012a; Mahmoudkhani and Langer, 2002). The angle values at phosphor atom from 106.23 (13) to 113.67 (12)° are otherwise not exceptional and show a distorted tetrahedral geometry for the methylphosphonate anion as expected. In the crystal, chains are connected through O—H...O hydrogen bonding interactions involving water molecules and oxyanions giving rise to a supramolecular two dimensional structure depicted in Fig.4.

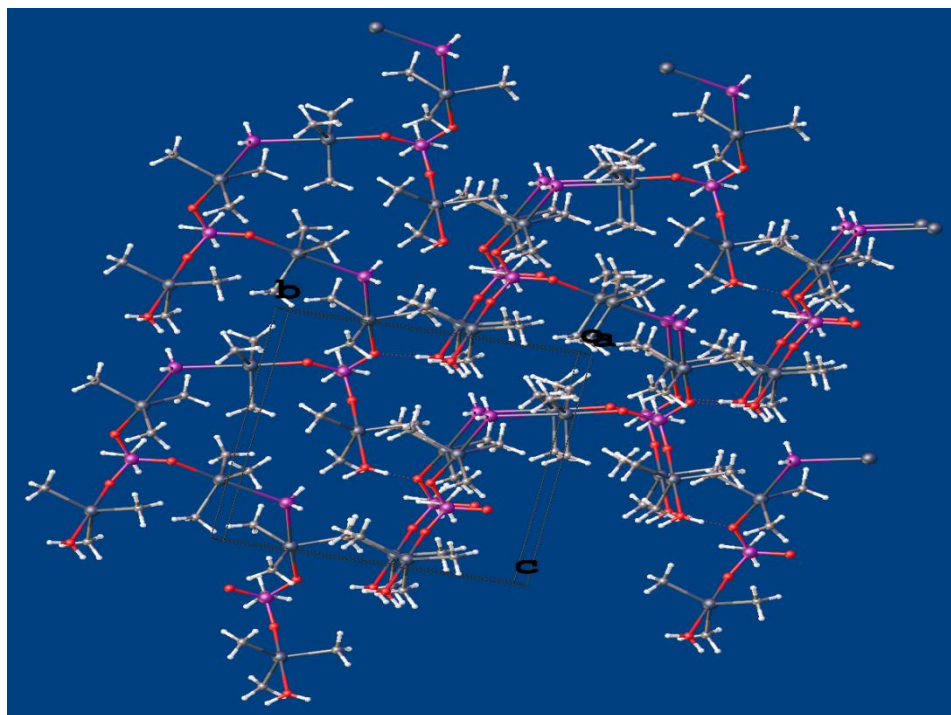


**Fig 4:-**3D structure of **1** showing 50% probability ellipsoids.

Crystals of **2** were investigated by FT-IR spectroscopy in ATR mode. FT-IR data evidence absorption bands that can be assigned to hydrogenphosphonate and SnPh<sub>3</sub> moiety. The vibration bands located at 1132 and 1109 cm<sup>-1</sup> are assigned to νPO<sub>3</sub><sup>2-</sup> (Nakamoto, 1997). Vibration bands, characteristic of phenyl ligands, are observed at 735 and 697 cm<sup>-1</sup> corresponding to δ(Csp<sup>2</sup>-H) and δ(C = C) elongations, respectively. The Mössbauer parameters show two different tin centres: the quadrupole splitting values of 2.84 mm.s<sup>-1</sup> and 2.51 mm.s<sup>-1</sup> indicate a trigonal bipyramidal and a tetrahedral arrangement at tin atom, respectively (Bancroft and Platt, 1972; Parish, 1984).

The compound **2** crystallizes in the monoclinic P2<sub>1</sub>/n space group as clear light colourless block-like crystal. There are one hydrogenphosphonate ion and two [SnPh<sub>3</sub>]<sup>+</sup> moieties in the molecular structure which view is shown in Fig. 5. The structure of **2** corresponds to an infinite anionic chain of [HPO<sub>3</sub>(SnPh<sub>3</sub>)]<sup>-</sup> with bridging hydrogenphosphonate anions and [SnPh<sub>3</sub>]<sup>+</sup> moieties connected to the chain *via* the third remaining hydrogenphosphonate oxygen atoms through Sn—O bonds (Fig. 5).



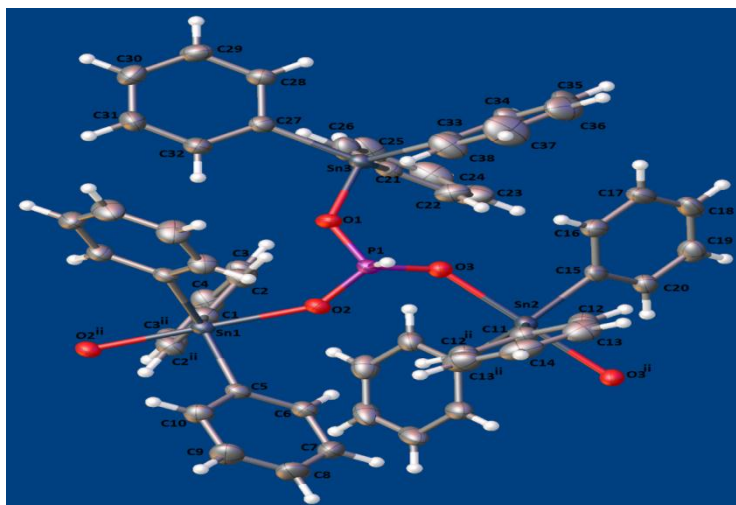


**Fig 5:-**Molecular structure of HPO<sub>3</sub>(SnPh<sub>3</sub>) (**2**) showing 50% probability ellipsoids and the crystallographic numbering scheme.

Thus, the hydrogenphosphonate dianion behaves as a tri O-coordinating ligand. There are two types of SnPh<sub>3</sub>; a *trans*-coordinated one, the environment around the tin(IV) atom being trigonal bipyramidal (tbp) and a monocoordinated one, the environment around the Sn(IV) centre being tetrahedral (td) (Figs. 6 and 7). In the *trans*-coordinated SnPh<sub>3</sub> moiety, the phenyl groups occupy the equatorial positions. The tin centres around each hydrogenphosphonate are differently coordinated by this last.

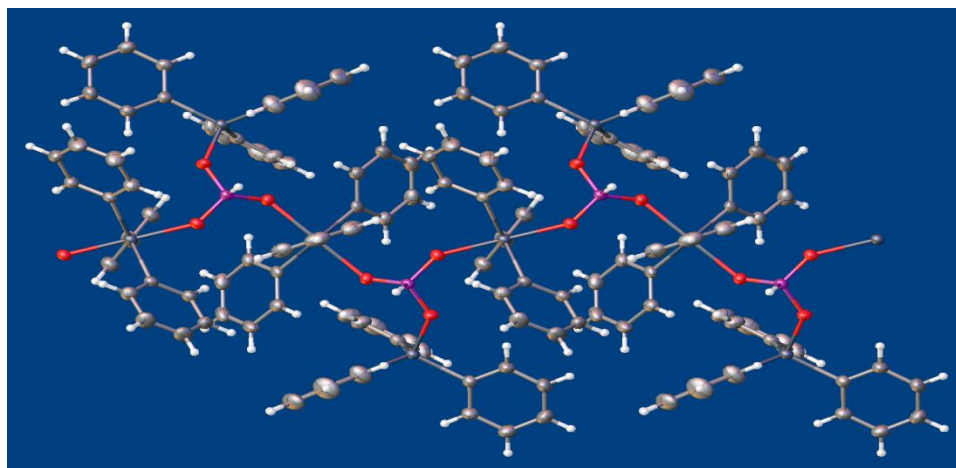


**Fig 6:-**Molecular structure of **2** showing the infinite ionic chain and [SnPh<sub>3</sub>]<sup>+</sup> cations set on. Ellipsoids are drawn at 50% probability.

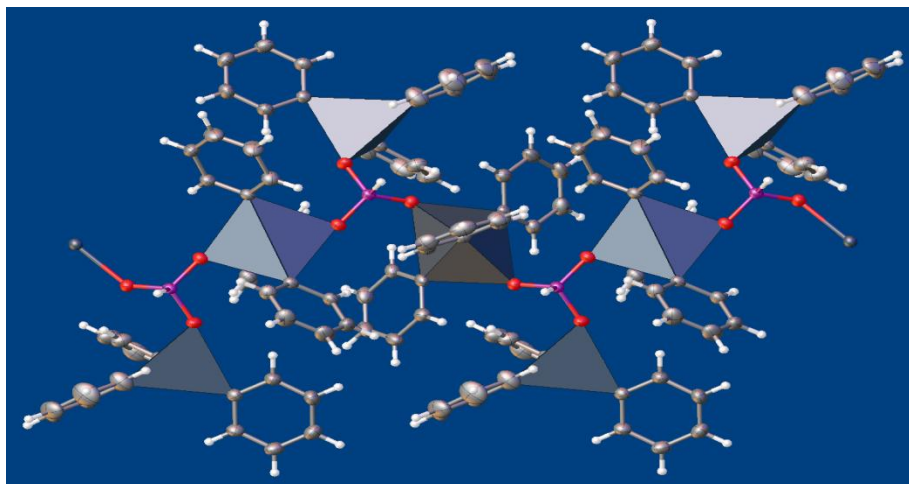


**Fig 7:**-Molecular structure of **2** showing the two polyhedron types at tin atoms. Ellipsoids are drawn at 50% probability.

The sum of the angles at tin about the *trans*-coordinated  $\text{SnPh}_3$  moieties are equal to  $360^\circ$  indicating a perfect planar  $\text{SnC}_3$  group. The angle values at the Sn centre for the monocoordinated  $\text{SnPh}_3$  moieties from  $99.28$  (11) to  $116.18$  (12) $^\circ$  indicate a distorted tetrahedron around Sn3 atom. The Sn—C distances are in the range of those found in *tbp* and *td*  $\text{SnPh}_3$  moieties (Diop *et al.*, 2013a, 2012a, 2011b). In the *trans*-coordinated moieties the apical positions of each  $\text{SnC}_3\text{O}_2$  framework are occupied by similar oxygen atoms of the hydrogenphosphonates [Sn1—O2 2.196 (2); Sn2—O3 2.242 (2) Å]; these distance values are higher than the Sn—O distance (2.001 (2) Å) in the tetrahedral arrangement. The O—Sn—O angles [O2<sup>i</sup>—Sn1—O2 177.03 (12) and O3<sup>ii</sup>—Sn2—O3 178.22 (13) $^\circ$ ] reveal a slight deviation from linearity. The P—O distances [1.502 (2), 1.510 (2) and 1.553 (2) Å] are in the range of those found in the literature (Larrea *et al.*, 2016; Ouarsal *et al.*, 2016; Hamchaoui *et al.*, 2013a, 2013b; Oh and Burns, 2014; Berrocal *et al.*, 2014). The P—H bond distance of 1.42 (4) is in the range of those found in the literature (Ouarsal *et al.*, 2016; Hamchaoui *et al.*, 2013a). The angle values at phosphor atom from  $103.2$  (17) to  $115.16$  (13) $^\circ$  show a distorted tetrahedral geometry in the hydrogenphosphonate anion as expected. In the crystal of complex **2**, chains are arranged within the lattice (Fig. 8).

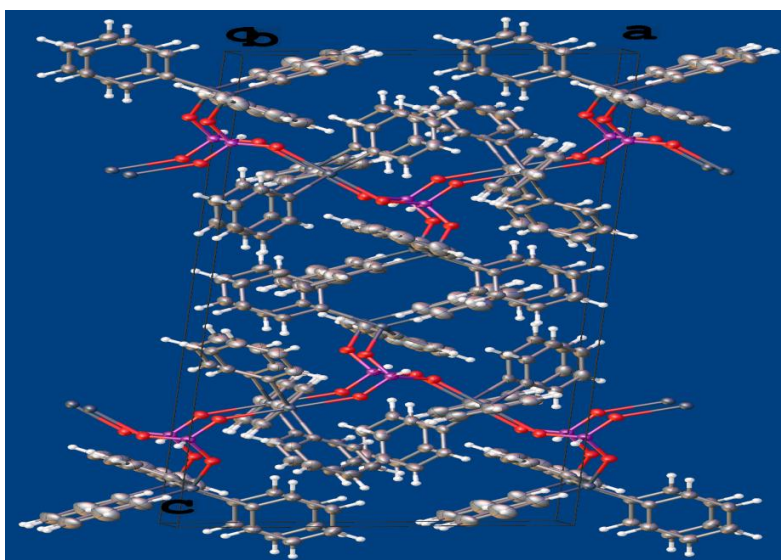


**Fig 8:**-Packing diagram of **2** showing 50% probability ellipsoids.

### Conclusion:-

In this work, the studied triorganotin(IV) phosphonates **1** and **2** describe an ionic infinite chain connected to  $\text{SnR}_3$  residues. In the case of the structure of **1**, the tin atom about the  $\text{SnR}_3$  moiety is coordinated to an O water molecule. Thus, the main difference between the structures is that in **1**, all tin atoms are at the centre of a trigonal bipyramidal

polyhedron while **2** exhibits two polyhedra types: a trigonal bipyramidal polyhedron within the chain and, a tetrahedron for the  $\text{SnR}_3$  moiety set on the chain. In **1**, the water molecule is involved in inter-chains hydrogen bonding interactions, enabling to grow a 3D structure. In contrast, in **2**, chains stacking expand within the lattice. In both structures the phosphonate anion behaves as a tri-O-coordinating ligand towards tin centres. The infrared and mössbauer spectroscopic characterization presents somewhat a little limit, for instance the difference between the two present trigonal bipyramidal polyhedra in **1**. Completion of the studies with single crystal X-ray diffraction highlighted this coordination. Further works in investigation of other triorganotin(IV) phosphonate compounds with or without a  $\text{PH}_2$  bridge are in progress.

### Acknowledgment:-

We thank Professor B. Mahieu, University of Louvain-La-Neuve, Belgium, Professor José Domingos Ardisson, Centro de Desenvolvimento da Tecnologia Nuclear (CDTN), Serviço de Nanotecnologia (SEANAN), Laboratório de Física Aplicada, Pampulha, Belo Horizonte, Brazil, Dr. Arnaud Grosjean, Institut de Chimie de la Matière Condensée, Université de Bordeaux, France and Dr. Laurent Plasseraud, Institut de Chimie Moléculaire, Université de Bourgogne Franche-Comté, Dijon, France for equipment support.

### References:-

1. Bao, S.-S. and Zheng, L.-M. (2016): Magnetic materials based on 3d metal phosphonates. *Coord. Chem. Rev.*, 319: 63–85.
2. Hamchaoui, F., Alonzo, V., Venegas-Yazigi, D., Rebbah, H. and LeFur, E. (2013a): Six novel transition-metal hydrogenphosphonate compounds, with structure related to yavapaiite: Crystal structures and magnetic and thermal properties of  $\text{A}^{\text{I}}[\text{M}^{\text{III}}(\text{HPO}_3)_2]$  (A=K,  $\text{NH}_4$ , Rb and M=V, Fe). *J. Solid State Chem.*, 198: 295–302.
3. *Metal Phosphonate Chemistry: From Synthesis to Applications*, Editors A. Clearfield and K. Demadis, the Royal Society of Chemistry, 2012.
4. Mao, J.-G. (2007): Structures and luminescent properties of lanthanide phosphonates. *Coord. Chem. Rev.*, 251: 1493–1520.
5. Fernandez-Armas, S., Mesa, J. L., Pizarro, J. L., Pena, A., Chapman, J. P. and Arriortua, M. I. (2004a): Hydrothermal synthesis, crystal structure and spectroscopic and magnetic properties  $(\text{C}_2\text{H}_{10}\text{N}_2)[\text{Mn}_{2.09}\text{Co}_{0.91}(\text{HPO}_3)_4]$ . *Mat. Res. Bull.*, 39: 1779–1790.
6. Mallouk, T. E., Kim, H. N., Oliver, P. J. and Keller, S. W. (1996): *Comprehensive Supramolecular Chemistry*, Edited by G. Alberti & T. Bein, Pergamon, New York, 7.
7. Cao, G., Hong, H. G. and Mallouk, T. E. (1992): Layered metal phosphates and phosphonates: from crystals to monolayers. *Acc. Chem. Res.*, 25(9): 420–427.
8. Etaiw, S. E. H., Abd El-Aziz, D. M. and Ali, E. A. (2019): Crystal structure, cytotoxicity and biological activity of hydrogen bonded networks based on dimethyltin (IV) and bipodal ligands. *J. Organomet. Chem.*, 894: 43–60.
9. Mao, W., Bao, K., Feng, Y., Wang, Q., Li, J. and Fan, Z. (2015): Synthesis, crystal structure, and fungicidal activity of triorganotin(IV) 1-methyl-1H-imidazole-4-carboxylates. *Main Group Met. Chem.*, 38: 27–30.
10. Devendra, R., Edmonds, N. R. and Sohnel, T. (2015): Organotin carboxylate catalyst in urethane formation in a polar solvent: an experimental and computational study. *RSC Adv.*, 5: 48935–48945.
11. Carraher, C. E., Roner, M. R., Frank, J., Slawek, P., Mosca, F., Shahi, K., Moric-Johnson, A. and Miller, L. (2019). Organotin Polymers for the Control of Pancreatic Cancer, OBM Hepatology and Gastroenterology. 3(2):doi:10.21926/obm.hg.1902019.
12. Carraher, C., Roner, M., Lynch, M., Moric-Johnson, A., Miller, L., Slawek, P., Mosca, F. and Frank, J. (2018). Organotin poly(ester ethers) from salicylic acid and their ability to inhibit human cancer cell lines, *Journal of Clinical Research in Oncology*. 1(1):1-11.
13. Roner, M., Shahi, K., Battin, A., Barot, G. and Arnold, T. (2014). Organotin Polymers As Chemotherapeutic Agents: Breast and Pancreatic Cancers, *Journal of Polymer Materials*. 31(1):1-14.
14. Troev, K. D. (2006): *Chemistry and Application of H-phosphonates*, Edited by Elsevier, Chapter 5, pp. 253–284.
15. Mahmoudkhani, A. H. and Langer, V. (2002): Structural correlations in methylphosphonate and hydrogenphosphonate salts: crystal structures of anilinium and ethylenediammonium methylphosphonates. *J. Mol. Struct.*, 609: 55–60.
16. Fleck, M., Tillmanns, E. and Haussiih, S. (2000): Crystal structure of ethylenediammonium hydrogenphosphite,  $(\text{C}_2\text{N}_2\text{H}_8)(\text{H}_3\text{PO}_3)_2$ . *Z. Kristallogr. NCS*, 215(1): 109–110.

17. Paixao, J. A., Matos Beja, A., Silva, M. R. and Martin-Gil, J. (2000): Two anilinium salts: anilinium hydrogenphosphite and anilinium hydrogenoxalate hemihydrate. *Acta Crystallogr.*, C56: 1132–1135.
18. Hönlle, W., Walz, L. and von Schnering, H. G. (1990): Ethylenediammonium Hydridotrioxophosphate(2-)  $[H_3NCH_2CH_2NH_3PHO_3]$ . *Z. Naturforsch.*, B45: 1251–1254.
19. Ouarsal, R., Lachkar, M., Dusek, M., Albert, E. B., Castelló, J. B. C. and El Bali, B. (2016): Crystal structure of  $NaCd(H_2PO_3)_3 \cdot H_2O$  and spectroscopic study of  $NaM(H_2PO_3)_3 \cdot H_2O$ ,  $M = Mn, Co, Ni, Zn, Mg$  and  $Cd$ . *Polyhedron*, 106: 132–137.
20. Larrea, E. S., Mesa, J. L., Legarra, E., Aguayo, A. T. and Arriortua, M. I. (2016): Crystal structure of  $K_{0.75}[Fe^{II}_{3.75}Fe^{III}_{1.25}(HPO_3)_6] \cdot 0.5H_2O$ , an open-framework iron hydrogenphosphonate with mixed-valent  $Fe^{II}/Fe^{III}$  ions. *Acta Crystallogr.*, E72: 63–65.
21. Berrocal, T., Mesa, J. L., Larre, E. and Arrieta, J. M. (2014): Crystal structure of  $(NH_4)_2[Fe^{II}_5(HPO_3)_6]$ , a new open-framework hydrogenphosphonate. *Acta Crystallogr.*, E70: 309–311.
22. Oh, G. N. and Burns, P. C. (2014): Solid-state actinide acid hydrogenphosphonates from phosphorous acid melts. *J. Solid State Chem.*, 215: 50–56.
23. Hamchaoui, F., Rebbah, H. and LeFur, E. (2013b): Ammonium diphosphitoindate(III). *Acta Crystallogr.*, E69: i21–i22.
24. Li, H., Zhang, L., Liu, L., Jiang, T., Yu, Y., Li, G., Huo, Q. and Liu, Y. (2009): Organic template-directed indium hydrogenphosphonate-oxalate hybrid material: Synthesis and characterization of a novel 3D  $[C_6H_{14}N_2][In_2(HPO_3)_3(C_2O_4)]$  compound with intersecting channels. *Inorg. Chem. Commun.*, 12: 1020–1023.
25. Fernandez-Armas, S., Mesa, J. L., Pizarro, J. L., Lezama, L., Arriortua, M. I. and Rojo, T. (2004b): A new organically templated gallium(III)-doped chromium(III) fluorohydrogenphosphonate,  $(C_2H_{10}N_2)[Ga_{0.98}Cr_{0.02}(HPO_3)F_3]$  hydrothermal synthesis, crystal structure and spectroscopic properties. *J. Solid State Chem.*, 177: 765–771.
26. Diop, C. A. K., Diop, L. and Russo, U. (1999):  $(Ph_3Sn)_2A'$  ( $A' = O_4C_2, O_3Se, O_3PH, O_3AsPh, O_3PCH_3$  and  $(Ph_3Sn)_3O_4P$ : Synthesis, Mössbauer, IR and NMR studies. *Main Group Met. Chem.*, 22(4): 217–220.
27. Diop, T., Diop, L., Fall, D. and van der Lee, A. (2012a): Dibutylammonium bis(hydrogen methylphosphonato- $\kappa O$ )triphenylstannate(IV). *Acta Crystallogr.*, E68: m1284–m1285.
28. Driess, M., Merz, K. and Monsé, C. (2003): Synthesis of the first fluoro(phosphanyl)- and diphosphanyl-stannanes and surprising formation of  $[P(SnMe_3)_4]+SiF_5^-$ . *Chem. Commun.*, 2608–2609.
29. Martens, R., du Mont, W.-W., Jeske, J., Jones, P.G., Saak, W. and Pohl, S. (1995): Zum reaktionsverhalten von dialkyl(trichlorsilyl)phosphanen - verglichen mit trimethylsilylphosphanen - gegenüber dichlordimethylstannan: Austauschreaktionen und strukturen cyclischer chlorstannylphosphan-dichlordimethylstannan-addukte. *J. Organomet. Chem.*, 501(1-2): 251–261.
30. Hanssgen, D., Aldenhoven, H. and Nieger, M. (1990): Ein neues PH- funktionelles Diphosphadistannetan:  $(tBu_2SnPH)_2$ . *Chem. Ber.*, 123: 1837–1839.
31. Diop, T., Diop, L., Kociock-Köhn, G., Molloy, K. C. and Ardisson, J. D. (2013a): Synthesis, spectroscopic characterization and crystal and molecular structures of phenylphosphonato  $SnR_3$  ( $R = Ph, Me$ ) derivatives. *Main Group Met. Chem.*, 36(1-2): 29–34.
32. Diop, T., Diop, L., Michaud, F. and Ardisson, J. D. (2013b):  $Et_4N[NO_3(SnClPh_3)_2(SnPh_3NO_3)]$ : a trinuclear organostannate complex and related derivatives. *Main Group Met. Chem.*, 36(3-4): 83–88.
33. Diop, T., Diop, L., Da Silva, J. G. and Fall, D. (2012b): Supramolecular architecture in crystalline  $Bu_2NH_2(PhPO_3H)_2SnMe_3$ . *Main Group Met. Chem.*, 35(1-2): 63–65
34. Diop, T., Diop, L., Diop, C. A. K., Molloy, K. C. and Kociock-Köhn, G. (2011a): Dicyclohexylammonium trimethylbis(hydrogen phenylphosphonato)stannate(IV). *Acta. Crystallogr.*, E67: m1872–m1873.
35. Diop, T., Diop, L., Molloy, K. C., Kociock-Köhn, G. and Stoeckli-Evans, H. (2011b): catena - Poly[[triphenyltin(IV)]- $\mu$ -phenylphosphinato- $\kappa 2O:O'$ ]. *Acta. Crystallogr.*, E67: m1674–m1675.
36. Ribot, F., Sanchez, C., Biesemans, M., Mercier, F. A. G., Martins, J. C., Gielen, M. and Willem, R. (2001): Di-n Butyltin methyl and phenylphosphonates, *Organometallics*, 20: 2593–2603.
37. Adair, B., Natarajan, S. and Cheetham, A. K. (1998): Synthesis and structural characterization of a novel tin(II) phosphonate,  $Sn_2(O_3PCH_3)(C_2O_4)$ . *Journal of Materials Chemistry*, 8(6): 1477–1479.
38. Chandrasekhar, V., Baskar, V. and Vittal, J. J. (2003): A New Structural Form of Tin in a Double O-Capped Cluster. *J. Am. Chem. Soc.*, 125: 2392–2393.
39. Chandrasekhar, V., Baskar, V., Gopal, K. and Vittal, J. J. (2005): Organooxotin Cages,  $\{[(n-BuSn)_3(\mu_3-O)(OC_6H_4-4-X)_3]_2[HPO_3]_4\}$ ,  $X = H, Cl, Br, \text{ and } I$ , in Double O-Capped Structures: Halogen-Bonding-Mediated Supramolecular Formation. *Organometallics*, 24: 4926–4932.

40. Mairychova, B., Stepnicka, P., Ruzicka, A., Dostal, L. and Jambor, R. (2014): Reactivity Studies on an Intramolecularly Coordinated Organotin(IV). *Organometallics*, 33(12): 3021–3029.
41. Bouâlam, M., Willem, R., Biesemans, M., Mahieu, B., Meunier-Piret, J. and Gielen, M. (1991): Synthesis, characterization and in vitro antitumor activity of diorganotin derivatives of substituted salicylic acids and analogs. Crystal structure of Bis(5-methoxysalicylato-di-n-butyltin)oxide. *Main Group Met. Chem.*, 14: 41–56.
42. Nonius (2003). COLLECT. Nonius BV, Delft, The Netherlands.
43. Otwinowski, Z. and Minor, W. (1997): *Methods in Enzymology. Macromolecular Crystallography, Part A*, Edited by C. W. Carter Jr & R. M. Sweet, New York: Academic Press, 276: pp. 307–326.
44. Sheldrick, G. M. (2008): A short history of *SHELX*. *Acta Crystallogr.*, A64: 112–122.
45. Dolomanov, O. V., Bourhis, L. J., Gildea, R. J., Howard, J. A. K. and Puschmann, H. (2009): OLEX2: a complete structure solution, refinement and analysis program. *J. Appl. Crystallogr.*, 42: 339–341.
46. Macrae, C. F., Bruno, I. J., Chisholm, J. A., Edgington, P. R., McCabe, P., Pidcock, E., Rodriguez-Monge, L., Taylor, R., van de Streek, J. and Wood, P. A. (2008): Mercury CSD 2.0 – new features for the visualization and investigation of crystal structures. *J. Appl. Crystallogr.*, 41: 466–470.
47. Apex2, Crystallographic Software, Suite, Bruker AXS Inc., Madison, Wisconsin (USA) 2013.
48. Saint (version 8.35A-2013), Area Detector Integration Software, Bruker AXS Inc., Madison, Wisconsin (USA) 2013.
49. Krause, L., Herbst-Irmer, R., Sheldrick, G. M. and Stalke, D. (2015): Comparison of silver and molybdenum microfocus X-ray sources for single-crystal structure determination. *J. Appl. Crystallogr.*, 48: 3–10.
50. Nakamoto, K. (1997): *Infrared and Raman Spectra of Inorganic and Coordination Compounds*, Edited by John Wiley and Sons, 5th Edition.
51. Bancroft, G. M. and Platt, R. H. (1972): Mössbauer spectra of inorganic compounds: Bonding and structure, *Advances in Inorganic Chemistry and Radiochemistry*, Edited by H. J. Emeleus and A. G. Sharpe, Academic Press, New York, 15, pp. 59–258.
52. Parish, R. V. (1984): "Structure and bonding in tin compounds" in "Mössbauer spectroscopy applied to inorganic chemistry", G. L. Lond Ed., Plenum Press, New York, 1, pp. 530.
53. Diop, M. B., Diop, L., Plasseraud, L. and Maris, T. (2015): Crystal structure of 2-methyl-1H-imidazol-3-ium aquatriflorido(oxalato- $\kappa^2$ O,O')stannate(IV). *Acta Crystallogr.*, E71: 520–522.